IEEE Access
Multidisciplinary | Rapid Review | Open Access Journal

Received November 17, 2017, accepted December 31, 2017, date of publication January 15, 2018,
date of current version February 28, 2018.

Digital Object Identifier 10.1109/ACCESS.2018.2791989

On Bit Error Probability and Power Optimization in Multihop Millimeter Wave Relay Systems

ALI CHELLI[1], (Member, IEEE), KIMMO KANSANEN[1], (Member, IEEE), MOHAMED-SLIM ALOUINI[2], (Fellow, IEEE), AND ILANGKO BALASINGHAM[1], (Senior Member, IEEE)

[1]Department of Electronics and Telecommunications, Norwegian University of Science and Technology, 7491 Trondheim, Norway
[2]Computer, Electrical, and Mathematical Science and Engineering Division, King Abdullah University of Science and Technology, Thuwal 23955, Saudi Arabia

Corresponding author: Ali Chelli (ali.chelli@iet.ntnu.no)

ABSTRACT 5G networks are expected to provide gigabit data rate to users via the millimeter-wave (mmWave) communication technology. One of the major problems faced by mmWaves is that they cannot penetrate buildings. In this paper, we utilize multihop relaying to overcome the signal blockage problem in an mmWave band. The multihop relay network comprises a source device, several relay devices, and a destination device and uses device-to-device communication. Relay devices redirect the source signal to avoid the obstacles existing in the propagation environment. Each device amplifies and forwards the signal to the next device, such that a multihop link ensures the connectivity between the source device and the destination device. We consider that the relay devices and the destination device are affected by external interference and investigate the bit error probability (BEP) of this multihop mmWave system. Note that the study of the BEP allows quantifying the quality of communication and identifying the impact of different parameters on the system reliability. In this way, the system parameters, such as the powers allocated to different devices, can be tuned to maximize the link reliability. We derive exact expressions for the BEP of M-ary quadrature amplitude modulation and M-ary phase-shift keying in terms of multivariate Meijer's G-function. Due to the complicated expression of the exact BEP, a tight lower bound expression for the BEP is derived using a novel Mellin-approach. Moreover, an asymptotic expression for the BEP at high SIR regime is derived and used to determine the diversity and the coding gain of the system. In addition, we optimize the power allocation at different devices subject to a sum power constraint such that the BEP is minimized. Our analysis reveals that optimal power allocation allows achieving more than 3-dB gain compared with the equal power allocation. This paper can serve as a framework for designing and optimizing mmWave multihop relaying systems to ensure link reliability.

INDEX TERMS Millimeter wave, device-to-device communication, bit error probability, multihop relaying, Nakagami-m fading.

I. INTRODUCTION

With the exponential growth in mobile traffic, network operators are required to increase the data rate offered to their customers. The main driving factor of the mobile traffic growth is the bandwidth-intensive media services. In 2017, the video traffic is expected to represent 67 % of the mobile traffic [1]. To meet the ever growing user demand, a lot of research effort has been invested in the last years in the fourth generation (4G) Long Term Evolution (LTE). Several techniques are used in 4G networks to boost the data rate provided to the end user. These techniques include network densification, heterogeneous network (HetNets), and carrier aggregation to name a few. Despite these efforts, 4G networks cannot support the expected growth in mobile traffic. Actually, by 2020 we foresee hundreds of times more traffic demand [1], which requires a move to the 5G era in order to meet the mobile customers requirements.

5G networks are expected to provide a minimum of 1 Gb/s data rate with uniform user experience [2]. Millimeter-wave (mmWave) communication represents the most effective solution to achieve the 5G vision [2]–[5]. In fact, the mmWave spectrum offers a huge underutilized band that can provide Giga-bit communication links. Nevertheless, several hurdles must be overcome to enable mmWave

communication to work properly. One of the major challenges faced by mmWave is that they cannot penetrate buildings and walls. Measurement results in [3] have shown that for a brick wall mmWave suffer a 178 dB attenuation. For two devices to communicate using mmWaves, they need to rely on a line-of-sight (LOS) link or reflection from buildings. If none of these conditions is satisfied, the mmWave signal is blocked due to shadowing and an outage event occurs [6], [7].

Signal outage may represent the bottleneck for mmWave communication in delivering uniform capacity for all users in the network. In order to deal with this problem, relaying techniques represent a promising solution to mmWave signal blockage [8]. We consider a typical device-to-device (D2D) communication scenario, where a source device sends data to a destination device over mmWave band without using the network infrastructure. In a real-world scenario, the propagation path of the signal between these two devices contains building walls, trees, and other types of objects. Bearing in mind that mmWaves cannot penetrate these objects, it is highly probable that the LOS link, between the source and the destination devices, is blocked. To overcome this problem, other devices laying in the propagation path between the transmitting and the receiving devices can be utilized to redirect the signal around the obstacles in the environment, such that a multihop communication link is created. The multihop link comprises the source device, the destination device, and multiple relay devices. Each of the relay devices amplifies and forwards the signal to the next device until it reaches the destination device. The data exchange between devices takes place using mmWave D2D communication.

In the literature, multihop relaying has been proposed to provide connectivity for mmWave networks in [8]. The authors investigate the performance of mmWave communication in indoor environment and analyze the effect of obstacles on the received signal strength using diffraction theory. A protocol that uses multihop relaying for mmWave communication is proposed and evaluated using system level simulations. Qiao *et al.* [9] use multihop relaying to remediate to the high path loss of mmWave signal. Thanks to multihop relaying the throughput can be significantly improved compared to the single hop solution. A metric for relay selection is proposed in [9] aiming to maximize the throughput while balancing the traffic load across the network. A multihop concurrent transmission scheme exploiting the spatial diversity of mmWaves is proposed.

A multihop routing protocol at mmWave frequencies is developed in [10]. The proposed protocol maximizes the sum quality of multiple video streams subject to a minimum quality constraint. In their study, Kim and Molisch [10] did not consider the impact of fast fading and interference on the system performance. Paper [11] addresses the same problem as in [10] while taking into account the impact of fast fading and interference on the system performance. In [12], a stochastic geometry approach has been proposed to study the connectivity in mmWave networks with multihop relaying. It is shown that the connectivity depends on the size and the density of obstacles and that multihop relaying can improve the connectivity versus the single hop mmWave strategy. In [4], the coverage of mmWave networks is studied using a stochastic geometry approach. The physical model used in [4] considers that the desirable signal follows a Nakagami-m distribution, while several interferers affect the communication link and each of these interferers is modeled using a Rayleigh distribution.

As opposed to all prior work on mmWave, this paper studies the bit error probability (BEP) of multihop mmWave relay systems in the presence of external interference and provides an exact expression for the BEP that is valid for a wide range of modulations schemes. The study of mmWave multihop amplify-and-forward relay systems is a challenging task. To address this problem, we propose the use of a novel Mellin approach to derive a lower-bound for the BEP. The tightness of this lower-bound is illustrated through numerical evaluations by comparing the exact BEP and its lower-bound. The investigation of the BEP allows quantifying the link quality of mmWave multihop relay systems and identifying the impact of the different parameters on the system reliability. The system parameters can then be tuned such that the link reliability is maximized. Following this line of thought, we derive an asymptotic expression for the BEP and exploit it to determine the optimal power allocation strategy that minimizes the BEP of multihop mmWave relay systems.

In this paper, we consider two devices communicating over the mmWave band. Due to path loss attenuation and obstacles blocking the LOS component between the transmitter and the receiver a single hop communication link cannot be established. To address this problem, the data is sent over N hops from the transmitter to the receiver. The mmWave network is composed of a source device S, a destination device D, and $N-1$ relay devices $R_n (n = 1, \ldots, N-1)$. Each relay amplifies the signal coming from the previous device and forwards it to the next device until it reaches the destination device. The data exchange in each hope uses D2D communication in the mmWave band. This D2D system can be regarded as a multihop amplify-and-forward (AF) relay network. In each hop, the mmWave signal undergoes a Nakagami fading channel. The relays and the destination devices are affected by L_n interferers. The interferers affecting a given device have independent identically distributed Nakagami fading.

In a first step, we derive the exact expression of the average BEP of the multihop relay system for M-ary quadrature amplitude modulation (M-QAM) and M-ary phase-shift keying (M-PSK) in terms of multivariate Meijer's G-function. This latter function is quite complex and does not give a clear insight on the behavior of the BEP. Therefore, we derive in a second step a lower-bound for the BEP. Towards this aim, an upper-bound for the end-to-end signal-to-interference ratio (SIR) is derived using the inequality between the harmonic mean and the geometric mean. The statistics of the SIR upper-bound are then computed and utilized to determine a lower-bound for the BEP.

The SIR upper-bound can be regarded as a product of rational power of ratio of Gamma random variables (RVs). Using *a novel Mellin-approach*, we derive closed-form expressions for the statistics of the SIR upper-bound. These statistics include the Mellin transform, the probability density function (PDF), the cumulative distribution function (CDF), and the moment generating function (MGF). Using the PDF of the product of the rational power of the ratio of Gamma RVs, a lower-bound for the BEP of M-QAM and M-PSK modulation schemes in multihop AF relaying systems is derived. An asymptotic expression for the BEP at high SIR regime is derived and used to determine the diversity and the coding gain of mmWave AF multihop systems. Moreover, we formulate the problem of optimal power allocation such that the system BEP is minimized subject to a sum power constraint. We show that this problem has a unique solution and derive the expression of the optimal power allocation at different nodes of the multihop relay network.

The rest of the paper is organized as follows. In Section II, we present the system model. The exact expression for the BEP is derived in Section III. Section IV is devoted for the Mellin transform and its main useful properties. Some preliminary results on the statistics of the product of rational power of the ratio of Gamma RVs are presented in Section V. Using the results of Section V, a lower-bound for the BEP is determined in Section VI. An asymptotic expression for the BEP is derived in Section VII. The problem of optimal power allocation subject to a sum power constraint is formulated and solved in Section VIII. Numerical results are illustrated and interpreted in Section IX. Finally, Section X draws the conclusion.

II. SYSTEM MODEL

We consider a multihop relay channel comprising a source device S, a destination device D, and $N-1$ relays $R_n (n = 1, \ldots, N-1)$ as illustrated in Fig. 1. The source and the destination devices are separated by several buildings blocking the LOS path. Since, mmWave signal cannot penetrate building walls, multihop relaying is utilized to redirect the mmWave signal around the obstacles and to establish a communication link between the source device and the destination device via D2D communication. The relay R_{n-1} amplifies and forwards the data generated by the source node to the relay R_n in the nth time slot. This process continues until the data reaches the destination device D in the Nth time slot. The fading channel between the relay R_{n-1} and R_n, denoted as h_n, follows a Nakagami distribution. The fading in different hops are independent non-identically distributed Nakagami distributions. Note that the Nakagami distribution is a well accepted model for small scale fading in mmWave [4], [13], [14].

We assume that the relay devices R_n and the destination device D are affected by $L_n (n = 1, \ldots, N)$ interferers. The fading channel between the ith interferer and relay R_n is referred to as $h_{In,i}$ and is Nakagami-m distributed. Note that the impact of interference on the coverage and the rate of

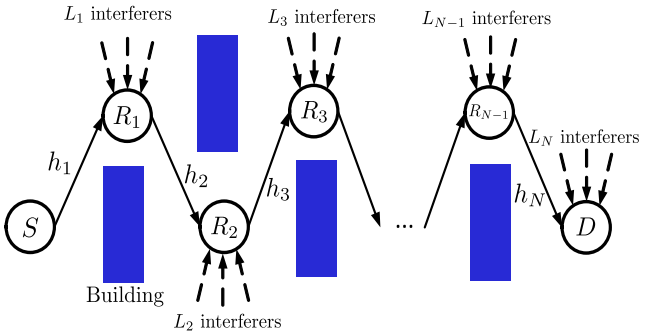

FIGURE 1. Multihop AF relaying with co-channel interference.

mmWave systems has been taken into account in [4], [13], and [14]. The interference has been assumed to follow a Nakagami distribution in [4], [13], and [14].

It has been shown in [13] that a dense mmWave network operates in interference-limited regime, whereas a sparse mmWave network operates in a power-limited regime. In this work, we consider a dense mmWave network characterized by its interference-limited regime. By definition, an interference-limited regime implies that the impact of noise is neglected compared to the impact of interference. Under the assumption of interference-limited regime, we can express the received signal at relay R_n as

$$y_n = h_n \sqrt{P_{n-1}} x_{n-1} + \sum_{i=1}^{L_n} \sqrt{P_{In,i}} h_{In,i} x_{In,i}, \tag{1}$$

where P_{n-1} is the power of the signal transmitted from the relay R_{n-1} and $P_{In,i}$ is the power of the ith interference signal affecting the relay node R_n. The terms x_{n-1} and $x_{In,i}$ stand for the transmitted symbols from the relay R_{n-1} and the ith interferer affecting R_{n-1}, respectively. It is reasonable to assume that the symbols $x_{In,i}$ are Gaussian distributed RVs with unity mean power.

In AF mode, the relay R_n amplifies the received signal y_n and forwards it to the relay R_{n+1}. The amplification factor at the relay R_n is denoted as G_n. The amplification process at the relay R_n consists of generating the signal $x_n = G_n y_n$.

A possible choice for the gain expression is

$$G_n^2 = \frac{1}{P_{n-1}|h_n|^2 + N_{0,n}}, \tag{2}$$

where $N_{0,n}$ is the noise variance. The choice of the amplification factor according to (2) allows limiting the output power if the fading amplitude of the preceding hop is low. However, this choice of the amplification factor makes the statistics of end-to-end SIR and the performance of the multihop relay system untractable. To cope with this problem an alternative choice of the amplification factor is proposed in [15] to be

$$G_n^2 = \frac{1}{P_{n-1}|h_n|^2}. \tag{3}$$

The amplification factor G_n in (3) is proportional to the inverse of the channel of the previous hop, regardless of the

interference in that hop. A drawback of the choice of the relay gain according to (3) is that it leads to high transmission power at relay R_n if the channel h_n in the previous hop is low. However, the choice of the relay gain as in (3) has several advantages: (i) this type of relay serves as a benchmark for practical AF multihop systems as mentioned in [15], (ii) at high SIR region, a similar performance is obtained for the AF multihop relaying system with the two relay gains (3) and (2), and (iii) the study of the performance of multihop AF relaying system becomes tractable if we choose the relay gain according to (3). Using the relay gain expression in (3) and utilizing a similar procedure as in [15], the end-to-end SIR is expressed as

$$\gamma_{\text{end}} = \left[\sum_{n=1}^{N} \frac{1}{\gamma_{\text{eq}\,n}}\right]^{-1}, \tag{4}$$

where

$$\gamma_{\text{eq}\,n} = \frac{P_{n-1}h_n^2}{\sum_{i=1}^{L_n} P_{In,i}h_{In,i}^2} = \frac{\gamma_n}{\gamma_{In}}. \tag{5}$$

The channel gain h_n follows a Nakagami-m distribution. Thus, $\gamma_n = P_{n-1}h_n^2$ is Gamma distributed with PDF given by

$$f_{\gamma_n}(\gamma) = \frac{m_n^{m_n}}{\bar{\gamma}_n^{m_n}\Gamma(m_n)}\gamma^{m_n-1}\exp\left(-\frac{m_n\gamma}{\bar{\gamma}_n}\right), \tag{6}$$

where $m_n \geq 1/2$ is a parameter describing the severity of fading for the nth hop (the link between the relays R_{n-1} and R_n) and $\Gamma(\cdot)$ stands for the Gamma function [16, eq. (8.310.1)]. The term $\bar{\gamma}_n = P_{n-1}\mathbb{E}(h_n^2)$ represents the average received power for the link between the source and the relay, where $\mathbb{E}(\cdot)$ is the expectation operator and $\mathbb{E}(h_n^2)$ is the variance of the fading channel for the nth hop.

Path loss models for mmWave signals have been proposed in [17] and [18] for 28 GHz and 38 GHz, respectively. Using these models, we can express the path loss experienced by the signal transmitted from relay R_{n-1} to relay R_n as

$$20\log_{10}\left(\frac{4\pi d_0}{\lambda}\right) + 10\eta\log_{10}\left(\frac{d_n}{d_0}\right), \tag{7}$$

where d_n refers to the distance between the relays R_{n-1} and R_n, d_0 is a free-space reference distance set to 5 meters in [17] and [18], λ stands for the wavelength (7.78 mm in 38 GHz and 10.71 mm in 28 GHz), and η represents the path loss exponent. Channel measurements in [17] and [18] have shown that the value of the path loss exponent η is equal to 2.2 in 38 GHz and 2.55 in 28 GHz. Using the path loss model for mmWaves in (7), we can obtain the expression of the channel variance of the nth hop as

$$\mathbb{E}(h_n^2) = \left(\frac{\lambda}{4\pi d_0}\right)^2\left(\frac{d_0}{d_n}\right)^{\eta}. \tag{8}$$

By setting $\alpha_n = m_n$ and $\beta_n = \bar{\gamma}_n/m_n$ in (6), we can rewrite the PDF of γ_n as

$$f_{\gamma_n}(\gamma) = \frac{\gamma^{\alpha_n-1}}{\beta_n^{\alpha_n}\Gamma(\alpha_n)}\exp\left(-\frac{\gamma}{\beta_n}\right). \tag{9}$$

Henceforth, we use the shorthand notation $X \sim \mathcal{G}(\alpha, \beta)$ to denote that the RV X follows a Gamma distribution with parameters α and β. From (9), we can write that $\gamma_n \sim \mathcal{G}(\alpha_n, \beta_n)$. The total interference at the relay $\gamma_{In} = \sum_{i=1}^{L_n} P_{In,i}h_{In,i}^2$ is the sum of L_n Gamma distributed RVs $P_{In,i}h_{In,i}^2$. We assume that $P_{In,i}h_{In,i}^2 (i = 1, \ldots, L_n)$ are independent identically distributed (i.i.d.) Gamma RVs with parameter a_n and b_n, i.e., $P_{In,i}h_{In,i}^2 \sim \mathcal{G}(a_n, b_n)$. It can easily be shown that the total interference γ_{In} is Gamma distributed with parameters $L_n a_n$ and b_n, i.e., $\gamma_{In} \sim \mathcal{G}(L_n a_n, b_n)$.

III. EXACT BIT ERROR PROBABILITY

In this section, we derive analytical expressions for the exact BEP of mmWave multihop relaying for different kind of modulation schemes. The BEP conditioned on the SIR γ_{end} of M-ary quadrature amplitude modulation (M-QAM) and M-ary phase-shift keying (M-PSK) is approximated as [19]

$$P_{e|\gamma_{\text{end}}} \approx a \cdot \exp(-b\,\gamma_{\text{end}}), \tag{10}$$

where the values of the parameters a and b are obtained using curve fitting techniques. For instance, by fitting the exact BEP curve for 16-QAM with the approximate expression in (10), the values of a and b, which have the minimum least square error for γ_{end} ranging from 0 to 30 dB are 0.0852 and 0.4030, respectively. The BEP in presence of fading is obtained by taking the expectation of the conditioned BEP $P_{e|\gamma_{\text{end}}}$ in (10) with respect to the SIR γ_{end} as

$$P_e = \mathbb{E}(P_{e|\gamma_{\text{end}}}) \approx \mathbb{E}(a \cdot \exp(-b\,\gamma_{\text{end}})), \tag{11}$$

where $\mathbb{E}(\cdot)$ denotes the expectation operator. Using the series expansion of the exponential function provided in [16, eq. (1.211.1)], we can express the BEP as

$$P_e = \mathbb{E}(P_{e|\gamma_{\text{end}}}) \approx a\sum_{k=0}^{\infty}\frac{(-1)^k b^k}{k!}\mathbb{E}(\gamma_{\text{end}}^k). \tag{12}$$

On the other hand, the moments of the instantaneous SNR is written in terms of the MGF of γ_{end}^{-1} using [16, eq. (3.381.4)] as

$$\mathbb{E}(\gamma_{\text{end}}^k) = \frac{1}{\Gamma(k)}\int_0^{\infty} M_{\gamma_{\text{end}}^{-1}}(t)t^{k-1}\,dt. \tag{13}$$

It follows that the BEP is determined as

$$\begin{aligned} P_e &= a\sum_{k=0}^{\infty}\frac{(-1)^k b^k}{k!}\mathbb{E}(\gamma_{\text{end}}^k) \\ &= a\sum_{k=0}^{\infty}\frac{(-1)^k b^k}{k!}\frac{1}{\Gamma(k)}\int_0^{\infty} M_{\gamma_{\text{end}}^{-1}}(t)t^{k-1}\,dt \\ &= a\int_0^{\infty} M_{\gamma_{\text{end}}^{-1}}(t)t^{-1}\sum_{k=0}^{\infty}\frac{(-1)^k b^k t^k}{k!\Gamma(k)}\,dt. \end{aligned} \tag{14}$$

Using [16, eq. (8.440)], the infinite sum in (14) is expressed as

$$\sum_{k=0}^{\infty} \frac{(-1)^k b^k t^k}{k!\Gamma(k)} = (bt)^{1/2} J_{-1}(2\sqrt{bt}), \tag{15}$$

where $J_{-1}(\cdot)$ is the Bessel function of the first kind and of order -1. Consequently, using (14) and (15) the BEP is obtained in a more compact form as

$$P_e = a \int_0^{\infty} M_{\gamma_{\text{end}}^{-1}}(t) b^{1/2} t^{-1/2} J_{-1}(2\sqrt{bt})\, dt. \tag{16}$$

Since $\gamma_{\text{end}}^{-1} = \sum_{n=1}^{N} \gamma_{\text{eq,n}}^{-1}$, the MGF $M_{\gamma_{\text{end}}^{-1}}(t)$ is obtained as

$$M_{\gamma_{\text{end}}^{-1}}(t) = \prod_{n=1}^{N} M_{\gamma_{\text{eq,n}}^{-1}}(t). \tag{17}$$

Utilizing [20, eq. (13)], the MGF of $\gamma_{\text{eq,n}}^{-1}$ is determined as

$$M_{\gamma_{\text{eq,n}}^{-1}}(t) = \frac{\Gamma(B_n)}{\Gamma(\alpha_n)} \Psi\left(A_n, 1-\alpha_n; \frac{t}{w_n}\right), \tag{18}$$

where $A_n = L_n a_n$, $B_n = L_n a_n + \alpha_n$, and $w_n = \frac{\beta_n}{b_n}$. For ease of notation, the symbols A_n, B_n, and w_n are utilized henceforth. The function $\Psi(\cdot,\cdot;\cdot)$ is the Tricomi confluent hypergeometric function defined in [16, eq. (9.211.4)]. Using (17) and (18), the MGF $M_{\gamma_{\text{end}}^{-1}}(t)$ is expressed as a product of N Tricomi hypergeometric functions as follows

$$M_{\gamma_{\text{end}}^{-1}}(t) = \prod_{n=1}^{N} \frac{\Gamma(B_n)}{\Gamma(\alpha_n)} \Psi\left(A_n, 1-\alpha_n; \frac{t}{w_n}\right). \tag{19}$$

Using [21, eq. (07.33.26.0004.01)], the Tricomi hypergeometric function $\Psi(a;b;z)$ can be expressed in terms of the Meijer's G-function $G_{p,q}^{m,n}(\cdot)$, defined in [21, eq. (07.34.02.0001.01)]. Thus, we can express the MGF $M_{\gamma_{\text{end}}^{-1}}(t)$ in terms of the Meijer's G-function as

$$M_{\gamma_{\text{end}}^{-1}}(t) = \prod_{n=1}^{N} \frac{\Gamma(B_n)}{\Gamma(\alpha_n)} G_{1,2}^{2,1}\left(\frac{t}{w_n}\middle| \begin{matrix} 1-A_n, \\ 0, \alpha_n, \end{matrix}\right). \tag{20}$$

With the help of [21, eq. (03.01.27.0006.01)] and [21, eq. (07.17.26.0007.01)], the Bessel function can also be written in terms of the Meijer's G-function as

$$J_{-1}\left(2\sqrt{bt}\right) = (bt)^{-1/2} G_{0,2}^{1,0}\left(bt\middle| \begin{matrix} , \\ 0, 1 \end{matrix}\right). \tag{21}$$

Substituting (20) and (21) in (16), we obtain

$$P_e = a \int_0^{\infty} \left[\prod_{n=1}^{N} \frac{\Gamma(B_n)}{\Gamma(\alpha_n)} G_{1,2}^{2,1}\left(\frac{t}{w_n}\middle| \begin{matrix} 1-A_n, \\ 0, \alpha_n, \end{matrix}\right)\right] t^{-1} G_{0,2}^{1,0}\left(bt\middle| \begin{matrix} , \\ 0, 1 \end{matrix}\right) dt \tag{22}$$

To compute the integral in (22), first, we replace each of the Meijer's G-functions in the first line of (22) by their contour integral representation using [21, eq. (07.34.02.0001.01)] which yields

$$\begin{aligned} P_e &= \frac{a}{(2\pi i)^N} \int_0^{\infty} \left[\prod_{n=1}^{N} \frac{\Gamma(B_n)}{\Gamma(\alpha_n)}\right] \int_{\mathcal{C}_1} \cdots \int_{\mathcal{C}_N} \prod_{n=1}^{N} \Gamma(-s_n) \\ &\quad \times \prod_{n=1}^{N} \left(\Gamma(\alpha_n - s_n)\Gamma(A_n + s_n)\left(\frac{t}{w_n}\right)^{s_n}\right) \\ &\quad \times ds_1 \cdots ds_N t^{-1} G_{0,2}^{1,0}\left(bt\middle| \begin{matrix} , \\ 0, 1 \end{matrix}\right) dt \\ &= \frac{a}{(2\pi i)^N} \left[\prod_{n=1}^{N} \frac{\Gamma(B_n)}{\Gamma(\alpha_n)}\right] \times \int_{\mathcal{C}_1} \cdots \int_{\mathcal{C}_N} \\ &\quad \times \prod_{n=1}^{N} \left(\Gamma(-s_n)\Gamma(\alpha_n - s_n)\Gamma(A_n + s_n)\left(\frac{1}{w_n}\right)^{s_n}\right) \\ &\quad \times \left[\int_0^{\infty} t^{\sum_{n=1}^{N} s_n - 1} G_{0,2}^{1,0}\left(bt\middle| \begin{matrix} , \\ 0, 1 \end{matrix}\right) dt\right] ds_1 \cdots ds_N, \end{aligned} \tag{23}$$

where $i = \sqrt{-1}$. In the last line of (23), the integral in brackets is evaluated with the help of [21, eq. (07.34.21.0009.01)] as follows

$$\int_0^{\infty} G_{0,2}^{1,0}\left(bt\middle| \begin{matrix} , \\ 0, 1 \end{matrix}\right) t^{\sum_{n=1}^{N} s_n - 1} dt = \frac{\Gamma\left(\sum_{n=1}^{N} s_n\right) b^{-\sum_{n=1}^{N} s_n}}{\Gamma\left(-\sum_{n=1}^{N} s_n\right)}. \tag{24}$$

Thus, the BEP P_e is obtained as

$$\begin{aligned} P_e &= a \left[\prod_{n=1}^{N} \frac{\Gamma(B_n)}{\Gamma(\alpha_n)}\right] \frac{1}{(2\pi i)^N} \int_{\mathcal{C}_1} \cdots \int_{\mathcal{C}_N} \frac{\Gamma\left(\sum_{n=1}^{N} s_n\right)}{\Gamma\left(-\sum_{n=1}^{N} s_n\right)} \\ &\quad \times \prod_{n=1}^{N} (\Gamma(-s_n)\Gamma(\alpha_n - s_n)\Gamma(A_n + s_n)) \left(\frac{1}{bw_1}\right)^{s_1} \cdots \\ &\quad \left(\frac{1}{bw_N}\right)^{s_N} ds_1 \cdots ds_N = a \left[\prod_{n=1}^{N} \frac{\Gamma(B_n)}{\Gamma(\alpha_n)}\right] G_{2,0:(1,2);\ldots;(1,2)}^{0,1:(2,1);\ldots;(2,1)} \\ &\quad \times \left[\begin{matrix} (1,0) : 1-A_1; \ldots; 1-A_N; \\ \text{---} \quad : (0,\alpha_1); \ldots; (0,\alpha_N); \end{matrix} \frac{1}{bw_1}, \ldots, \frac{1}{bw_N}\right], \end{aligned} \tag{25}$$

where $G_{A,C:(B^{(1)},D^{(1)});\ldots;(B^{(r)},D^{(r)})}^{0,\lambda:(\mu^{(1)},\nu^{(1)});\ldots;(\mu^{(r)},\nu^{(r)})}[\cdot]$ is the multivariate Meijer's G-function whose expression is deduced from the expression of the multivariate H-function defined in [22, eq. (1.3)]. Note that the MATHEMATICA implementation of the bivariate Meijer's G-function is provided in [23]. Using similar methods as in [23], it is possible to implement the multivariate Meijer's G-function in MATHEMATICA.

IV. MELLIN TRANSFORM AND ITS PROPERTIES

The expression of the BEP in (25) is important since it allows evaluating accurately the reliability of mmWave multihop relay systems. However, it is difficult to get any insight on the error behavior from the expression of the BEP in (25)

due to the complicated expression of the multivariate Meijer's G-function. Therefore, we derive in Section VI an upper-bound expression for the BEP. Towards this end, this section presents first some background information about the Mellin transform and its properties.

A. DEFINITION OF MELLIN TRANSFORM AND INVERSE MELLIN TRANSFORM

Definition 1: The Mellin transform $\mathcal{M}_s(X)$ of a positive RV X with continuous PDF $f_X(x)$ is its moment of order $(s-1)$, i.e.,

$$\mathcal{M}_s(X) = \mathbb{E}\left(X^{s-1}\right) = \int_0^\infty x^{s-1} f_X(x) dx. \tag{26}$$

The reciprocal formula allows obtaining the PDF $f_X(x)$ of a RV X from its Mellin transform $\mathcal{M}_s(X)$ as

$$f_X(x) = \frac{1}{2\pi i} \int_{\mathcal{C}} x^{-s} \mathcal{M}_s(X) ds. \tag{27}$$

The key reason for the importance of the Mellin transform in studying the distribution of the product of independent RVs stems from the following result: If X and Y are independent positive RVs with continuous PDFs $f_X(x)$ and $f_Y(y)$, then it is well known from statistics theory that the PDF $U = XY$ is expressed as

$$f_U(x) = \int_0^\infty \frac{1}{y} f_X\left(\frac{x}{y}\right) f_Y(y) dy = f_X *_M f_Y, \tag{28}$$

where the notation $(*_M)$ refers to the convolution in the Mellin sense. In fact, the expression in (28) is a convolution in the Mellin sense of $f_X(x)$ and $f_Y(y)$ [24, eq. (3.4.3)]. More importantly, the Mellin transform of the convolution in (28) is the product of the Mellin transforms [24, eq. (3.4.2)], i.e.,

$$\mathcal{M}_s(U) = \mathcal{M}_s(f_X *_M f_Y) = \mathcal{M}_s(X)\mathcal{M}_s(Y). \tag{29}$$

In the sequel of this section, we present some important properties of the Mellin transform.

Lemma 1: Let a be a positive real number and X and Y two positive RVs, such that $Y = aX$. The Mellin transform of Y is expressed as $\mathcal{M}_s(Y) = a^{s-1}\mathcal{M}_s(X)$.

Proof: Using the definition of the Mellin transform in (26), we can express $\mathcal{M}_s(Y)$ as

$$\begin{aligned}\mathcal{M}_s(Y) &= \mathbb{E}\left(Y^{s-1}\right) = \mathbb{E}\left((aX)^{s-1}\right) = \mathbb{E}\left(a^{s-1}X^{s-1}\right) \\ &= a^{s-1}\mathbb{E}\left(X^{s-1}\right) = a^{s-1}\mathcal{M}_s(X).\end{aligned} \tag{30}$$

■

Lemma 2: Let Y be a positive RV given by $Y = X^\alpha$. Then the Mellin transform of Y is derived as $\mathcal{M}_s(Y) = \mathcal{M}_{\alpha s-\alpha+1}(X)$. In particular, if $\alpha = -1$, i.e., $Y = \frac{1}{X}$ then $\mathcal{M}_s(Y) = \mathcal{M}_{-s+2}(X)$.

Proof: Applying the definition of the Mellin transform in (26), we can write $\mathcal{M}_s(Y)$ as

$$\begin{aligned}\mathcal{M}_s(Y) &= \mathbb{E}\left(Y^{s-1}\right) = \mathbb{E}\left((X)^{\alpha(s-1)}\right) \\ &= \mathbb{E}\left((X)^{\alpha s-\alpha+1-1}\right) = \mathcal{M}_{\alpha s-\alpha+1}(X).\end{aligned} \tag{31}$$

■

Lemma 3: Let $X_1, \ldots, X_N$ be N independent positive RVs and Y a RV given by $Y = \prod_{n=1}^N X_n$. Then the Mellin transform of Y is derived as $\mathcal{M}_s(Y) = \prod_{n=1}^N \mathcal{M}_s(X_n)$.

Proof: Utilizing the definition of the Mellin transform in (26), we can write $\mathcal{M}_s(Y)$ as

$$\begin{aligned}\mathcal{M}_s(Y) &= \mathbb{E}\left(Y^{s-1}\right) = \mathbb{E}\left(\left(\prod_{n=1}^N X_n\right)^{s-1}\right) \\ &= \mathbb{E}\left(\prod_{n=1}^N X_n^{s-1}\right) = \prod_{n=1}^N \mathbb{E}\left(X_n^{s-1}\right) = \prod_{n=1}^N \mathcal{M}_s(X_n).\end{aligned} \tag{32}$$

■

Lemma 4: Let X_1 and X_2 be two independent positive RVs and Y a RV given by $Y = \frac{X_1}{X_2}$. Then the Mellin transform of Y is derived as $\mathcal{M}_s(Y) = \mathcal{M}_s(X_1)\mathcal{M}_{2-s}(X_2)$.

Proof: Utilizing Lemma 3, we can express $\mathcal{M}_s(Y)$ as

$$\mathcal{M}_s(Y) = \mathcal{M}_s\left(\frac{X_1}{X_2}\right) = \mathcal{M}_s(X_1)\mathcal{M}_s\left(\frac{1}{X_2}\right).$$

Using Lemma 2, we obtain $\mathcal{M}_s(\frac{1}{X_2}) = \mathcal{M}_{2-s}(X_2)$. Consequently, $\mathcal{M}_s(Y) = \mathcal{M}_s(X_1)\mathcal{M}_{2-s}(X_2)$. ■

V. PRELIMINARY STATISTICAL RESULTS

Theorem 1 (Mellin Transform of the Product of Rational Powers of Ratio of Gamma RVs): Let $\{X_n\}_{n=1}^N$ and $\{Y_n\}_{n=1}^N$ be $2N$ independent non identically distributed Gamma random variables with $X_n \sim \mathcal{G}(\alpha_n, \beta_n)$ and $Y_n \sim \mathcal{G}(a_n, b_n)$. Let Z be defined as the product of powers of ratio of X_n and Y_n, i.e.,

$$Z \triangleq \prod_{n=1}^N \left(\frac{X_n}{Y_n}\right)^{1/N}. \tag{33}$$

The Mellin transform of the random variable Z is obtained in closed-form as

$$\mathcal{M}_s(Z) = \prod_{n=1}^N \left(\frac{b_n}{\beta_n}\right)^{\frac{(1-s)}{N}} \frac{\Gamma\left(\alpha_n + \frac{(s-1)}{N}\right)\Gamma\left(a_n + \frac{(1-s)}{N}\right)}{\Gamma(\alpha_n)\Gamma(a_n)}. \tag{34}$$

Proof: See Appendix A. ■

Corollary 1 (The PDF of the Product of Rational Powers of ratio of Gamma RVs): The PDF of Z is expressed as

$$\begin{aligned}f_Z(x) = &\frac{N x^{-1}}{\prod_{n=1}^N \Gamma(\alpha_n)\Gamma(a_n)} \\ &\times G_{N,N}^{N,N}\left(\prod_{n=1}^N \left(\frac{b_n}{\beta_n}\right) x^N \middle| \begin{matrix} 1-a_1, \ldots, 1-a_N \\ \alpha_1, \ldots, \alpha_N \end{matrix}\right),\end{aligned} \tag{35}$$

where $G_{p,q}^{m,n}(\cdot)$ is the Meijer's G-function defined in [21, eq. (07.34.02.0001.01)].

Note that the Meijer's G-function is a standard built-in function available in most mathematical software packages, such as MATLAB and MATHEMATICA.

Proof: The PDF of Z is determined by computing the inverse Mellin transform of $\mathcal{M}_s(Z)$ provided in (34) as

$$f_Z(x) = \frac{1}{2\pi i}\int_{\mathcal{C}} \mathcal{M}_s(Z)x^{-s}ds = \frac{1}{2\pi i}\int_{\mathcal{C}} \prod_{n=1}^{N}\left(\frac{b_n}{\beta_n}\right)^{(1-s)/N} \times \frac{\Gamma\left(\alpha_n + \frac{(s-1)}{N}\right)}{\Gamma(\alpha_n)\Gamma(a_n)}\Gamma\left(a_n + \frac{(1-s)}{N}\right)x^{-s}ds. \quad (36)$$

Making the change of variable $r = \frac{s-1}{N}$, we can rewrite the PDF $f_Z(x)$ as

$$f_Z(x) = \frac{Nx^{-1}}{\prod_{n=1}^{N}\Gamma(\alpha_n)\Gamma(a_n)}\frac{1}{2\pi i}\int_{\mathcal{C}}\prod_{n=1}^{N}\left(\frac{b_n}{\beta_n}\right)^{-r}\Gamma(\alpha_n + r) \times \Gamma(a_n - r)\left(x^N\right)^{-r}dr = \frac{Nx^{-1}}{\prod_{n=1}^{N}\Gamma(\alpha_n)\Gamma(a_n)} \times G_{N,N}^{N,N}\left(\prod_{n=1}^{N}\left(\frac{b_n}{\beta_n}\right)x^N \middle| \begin{matrix}1-a_1,\ldots,1-a_N\\ \alpha_1,\ldots,\alpha_N\end{matrix}\right), \quad (37)$$

which is the desired result. ∎

Corollary 2 (The CDF of the Product of Rational Powers of Ratio of Gamma RVs): The CDF of Z is determined as

$$F_Z(x) = \frac{1}{\prod_{n=1}^{N}\Gamma(\alpha_n)\Gamma(a_n)}G_{N+1,N+1}^{N,N+1} \times \left(\prod_{n=1}^{N}\left(\frac{b_n}{\beta_n}\right)x^N \middle| \begin{matrix}1-a_1,\ldots,1-a_N,1\\ \alpha_1,\ldots,\alpha_N,0\end{matrix}\right). \quad (38)$$

Proof: Integrating the PDF expression in (35), the CDF $F_Z(x)$ is obtained

$$F_Z(x) = \int_0^x f_Z(z)dz = \frac{N}{\prod_{n=1}^{N}\Gamma(\alpha_n)\Gamma(a_n)}\frac{1}{2\pi i} \times \int_{\mathcal{C}}\prod_{n=1}^{N}\left(\frac{b_n}{\beta_n}\right)^{-r}\Gamma(\alpha_n + r)\,\Gamma(a_n - r) \times \left[\int_0^x z^{-Nr-1}dz\right]dr \quad (39)$$

Using the fact that $\int_0^x z^{-Nr-1}dz = \frac{x^{-Nr}}{-Nr}$ and that $-r = \frac{\Gamma(1-r)}{\Gamma(-r)}$, the expression of the CDF $F_Z(x)$ reduces to

$$F_Z(x) = \frac{1}{\prod_{n=1}^{N}\Gamma(\alpha_n)\Gamma(a_n)}\frac{1}{2\pi i}\int_{\mathcal{C}}\prod_{n=1}^{N}\left(\frac{b_n}{\beta_n}\right)^{-r}\frac{\Gamma(-r)}{\Gamma(1-r)} \times \Gamma(\alpha_n+r)\Gamma(a_n-r)\left(x^N\right)^{-r}dr = \frac{1}{\prod_{n=1}^{N}\Gamma(\alpha_n)\Gamma(a_n)} \times G_{N+1,N+1}^{N,N+1}\left(\prod_{n=1}^{N}\left(\frac{b_n}{\beta_n}\right)x^N \middle| \begin{matrix}1-a_1,\ldots,1-a_N,1\\ \alpha_1,\ldots,\alpha_N,0\end{matrix}\right). \quad (40)$$

∎

Corollary 3 (The MGF of the Product of Rational Powers of Ratio of Gamma RVs): The MGF of Z is obtained as

$$M_Z(t) = \frac{\sqrt{N}}{(2\pi)^{(N-1)/2}\prod_{n=1}^{N}\Gamma(\alpha_n)\Gamma(a_n)}G_{2N,N}^{N,2N} \times \left(\frac{\prod_{n=1}^{N}\left(\frac{b_n}{\beta_n}\right)^N N^N}{t^N}\middle| \begin{matrix}\Delta(N,1),1-a_1,\ldots,1-a_N,1\\ \alpha_1,\ldots,\alpha_N,0\end{matrix}\right) \quad (41)$$

where $\Delta(N,1) = \frac{1}{N},\frac{2}{N},\ldots,\frac{N}{N}$.

Proof: By applying the Laplace transform on the PDF expression in (35), the MGF in (41) is deduced with the help of [25, eq (3.40.1.1)]. ∎

VI. LOWER-BOUND ON THE BIT ERROR PROBABILITY

The exact expression for the end-to-end SIR is given by (4). In order to get a simpler expression for the BEP than (25), we need first to find an upper-bound for the end-to-end SIR γ_{end}. Towards this aim, we utilize the well known inequality between the geometric mean and the harmonic mean. Let $\mathcal{H}_N$ and $\mathcal{G}_N$ denote the harmonic mean and the geometric mean, respectively, for the variables $\gamma_{\text{eq},1},\ldots,\gamma_{\text{eq,N}}$. The harmonic mean $\mathcal{H}_N \triangleq N(\sum_{n=1}^{N}1/\gamma_{\text{eq,n}})^{-1}$, whereas the geometric mean $\mathcal{G}_N \triangleq \prod_{n=1}^{N}\gamma_{\text{eq,n}}^{1/N}$. Using (4) and the fact that $\mathcal{H}_N \leq \mathcal{G}_N$, we can obtain an upper-bound for the end-to-end SIR as

$$\gamma_{\text{end}} \leq \gamma_{\text{up}} = \frac{1}{N}\prod_{n=1}^{N}\gamma_{\text{eq,n}}^{1/N} = \frac{1}{N}\prod_{n=1}^{N}\left(\frac{\gamma_n}{\gamma_{In}}\right)^{1/N}. \quad (42)$$

We recall that γ_n and γ_{In} are both Gamma distributed with $\gamma_n \sim \mathcal{G}(\alpha_n,\beta_n)$ and $\gamma_{In} \sim \mathcal{G}(L_n a_n, b_n)$. Applying Theorem 1 and Lemma 1, the Mellin transform of γ_{up} is obtained as

$$\mathcal{M}_s(\gamma_{\text{up}}) = \prod_{n=1}^{N}\left(\frac{b_n}{\beta_n}\right)^{\frac{(1-s)}{N}}\left(\frac{1}{N}\right)^{s-1}\frac{\Gamma\left(\alpha_n + \frac{(s-1)}{N}\right)}{\Gamma(\alpha_n)} \times \frac{\Gamma\left(L_n a_n + \frac{(1-s)}{N}\right)}{\Gamma(L_n a_n)}. \quad (43)$$

Using the transformation of RVs, Corollary 1, and Corollary 2, we can determine the expressions of the PDF, the CDF, and the MGF of the upper-bound γ_{up} in closed-form as follows. The PDF expression is obtained as

$$f_{\gamma_{\text{up}}}(x) = \frac{Nx^{-1}}{\prod_{n=1}^{N}\Gamma(\alpha_n)\Gamma(L_n a_n)}G_{N,N}^{N,N} \times \left(\prod_{n=1}^{N}\left(\frac{b_n}{\beta_n}\right)(Nx)^N \middle| \begin{matrix}\Psi(1-L_n a_n)\\ \alpha_1,\ldots,\alpha_N\end{matrix}\right), \quad (44)$$

where $\Psi(1-L_n a_n) = 1-L_1\,a_1,\ldots,1-L_n a_n,\ldots,1-L_N a_N$. The CDF $F_{\gamma_{\text{up}}}(x)$ is determined as

$$F_{\gamma_{\text{up}}}(x) = \frac{1}{\prod_{n=1}^{N}\Gamma(\alpha_n)\Gamma(L_n a_n)}G_{N+1,N+1}^{N,N+1} \times \left(\prod_{n=1}^{N}\left(\frac{b_n}{\beta_n}\right)(xN)^N \middle| \begin{matrix}\Psi(1-L_n a_n),1\\ \alpha_1,\ldots,\alpha_N,0\end{matrix}\right). \quad (45)$$

$$M_{\gamma_{\rm up}}(t)=\frac{\sqrt{N}}{(2\pi)^{(N-1)/2}\prod_{n=1}^{N}\Gamma(\alpha_n)\Gamma(L_n a_n)}G_{2N,N}^{N,2N}\left(\frac{\prod_{n=1}^{N}\left(\frac{b_n}{\beta_n}\right)^{N}N^{NN}}{t^{N}}\middle|\begin{matrix}\Delta(N,1),1-a_1,\ldots,1-a_N,1\\ \alpha_1,\ldots,\alpha_N,0\end{matrix}\right). \tag{46}$$

The MGF $M_{\gamma_{\rm up}}(t)$ is evaluated as (46), as shown at the top of this page.

Using (44), we can derive a lower-bound $P_{e,\rm low}$ for the average BEP as

$$\begin{aligned}
&P_{e,\rm low}\\
&=\int_0^\infty P_{e|\gamma_{\rm up}}f_{\gamma_{\rm up}}(x)\,dx=\int_0^\infty\frac{a\exp(-bx)x^{-1}}{\prod_{n=1}^{N}\Gamma(\alpha_n)\Gamma(L_n a_n)}\\
&\quad\times G_{N,N}^{N,N}\left(\prod_{n=1}^{N}\left(\tfrac{b_n}{\beta_n}\right)(Nx)^{N}\middle|\begin{matrix}\Psi(1-L_n a_n)\\ \alpha_1,\ldots,\alpha_N\end{matrix}\right)dx\\
&=\int_0^\infty\frac{a\exp(-bx)}{\prod_{n=1}^{N}\Gamma(\alpha_n)}\frac{x^{-1}}{\prod_{n=1}^{N}\Gamma(L_n a_n)}\frac{1}{2\pi i}\int_{\mathcal{C}}\prod_{n=1}^{N}\left(\frac{b_n}{\beta_n}\right)^{-r}\\
&\quad\times\Gamma\left(L_n a_n-r\right)\Gamma\left(\alpha_n+r\right)(Nx)^{-Nr}dxdr\\
&=\frac{a}{\prod_{n=1}^{N}\Gamma(\alpha_n)\Gamma(L_n a_n)}\frac{1}{2\pi i}\int_{\mathcal{C}}\prod_{n=1}^{N}\left(\frac{b_n}{\beta_n}\right)^{-r}\\
&\quad\times\Gamma\left(\alpha_n+r\right)\Gamma\left(L_n a_n-r\right)\\
&\quad\times\left[\int_0^\infty\exp(-bx)x^{-1}(Nx)^{-Nr}dx\right]dr\\
&=\frac{a}{\prod_{n=1}^{N}\Gamma(\alpha_n)\Gamma(L_n a_n)}\frac{1}{2\pi i}\int_{\mathcal{C}}\prod_{n=1}^{N}\left(\frac{b_n}{\beta_n}\right)^{-r}\Gamma(\alpha_n+r)\\
&\quad\times\Gamma\left(L_n a_n-r\right)b^{Nr}\Gamma(-Nr)dr.
\end{aligned}\tag{47}$$

Using the Gauss multiplication formula [26, eq. (6.1.20)], we can write

$$\Gamma(-Nr)=(2\pi)^{\frac{1}{2}(1-N)}N^{-Nr-\frac{1}{2}}\prod_{k=0}^{N-1}\Gamma\left(\frac{k}{N}-r\right). \tag{48}$$

Utilizing (47) and (48), we can express the BEP as

$$\begin{aligned}
P_{e,\rm low}=&\frac{a}{\left(\sqrt{2\pi}\right)^{N-1}\sqrt{N}\prod_{n=1}^{N}\Gamma(\alpha_n)\Gamma(L_n a_n)}G_{2N,N}^{N,2N}\\
&\times\left(\prod_{n=1}^{N}\left(\tfrac{b_n}{\beta_n}\right)\left(\tfrac{N}{b}\right)^{N}\middle|\begin{matrix}\Psi(1-L_n a_n),\Theta\left(\frac{k}{N}\right)\\ \alpha_1,\ldots,\alpha_N\end{matrix}\right),
\end{aligned}\tag{49}$$

where $\Theta\left(\frac{k}{N}\right)=1,\ldots,1-\frac{k}{N},\ldots,1-\frac{N-1}{N}$.

Karagiannidis *et al.* [27] proposed bounds for the BEP of multihop AF relay networks over Nakagami fading. First, the end-to-end signal-to-noise ratio is upper-bounded using the inequality between the geometric and the harmonic means. The upper-bound is expressed as a product of rational powers of Gamma RVs. Karagiannidis *et al.* [27] derive the statistics of the upper-bound by first computing the MGF of the product of rational powers of Gamma RVs. This operation involves the computation of N-folds integral[1] which makes this task quite challenging. Once the MGF is determined, the expression of the PDF is deduced from it using the inverse Laplace transform. Utilizing this PDF, a lower-bound for the BEP is computed.

[1] N corresponds to the number of hops in the multihop relay network.

Our work differs from [27] in several aspects. We investigate in this paper multihop relaying for mmWave communication whereas [27] considers multihop relaying for traditional microwave frequencies. Moreover, as opposed to [27], we consider in our work the impact of interference on the performance of multihop relay networks over Nakagami channels which makes the addressed problem more general and more difficult to solve. For obtaining a BEP lower-bound for such kind of systems, we need first to derive the statistics of the product of rational power of the ratio of Gamma RVs. The MGF-approach proposed in [27] is not easy to apply for the problem considered in this paper. Therefore, we propose in this paper a novel Mellin-approach for evaluating the statistics of the product of rational power of the ratio of Gamma RVs. Note that the MGF-approach is very suitable for evaluating the statistics of the sum of RVs, whereas the Mellin-approach is well suited for the evaluation of the statistics of the product and the ratio of RVs this is mainly due to the properties of the Mellin transform [see Section IV].

VII. ASYMPTOTIC BIT ERROR PROBABILITY

In this section, we derive an asymptotic closed-form expression for the average BEP. This asymptotic expression allows to get an insight on the system performance as well as the impact of different system parameters on the BEP of multihop AF relay networks. The average BEP can generally be obtained by averaging the conditional error probability over the SIR, i.e.,

$$P_e=\int_0^\infty P_{e|\gamma_{\rm end}}f_{\gamma_{\rm end}}(x)\,dx, \tag{50}$$

where the expression of the conditional probability $P_{e|\gamma_{\rm end}}$ is provided in (10).

Using the expression of $\gamma_{\rm end}$ in (4), we can obtain an upper-bound $\gamma_{\rm up}$ for the end-to-end SIR $\gamma_{\rm end}$ as follows

$$\gamma_{\rm end}=\left[\sum_{n=1}^{N}\frac{1}{\gamma_{{\rm eq}\,n}}\right]^{-1}\leq\min(\gamma_{{\rm eq}\,1},\ldots,\gamma_{{\rm eq}\,N})=\gamma_{\rm up}. \tag{51}$$

In the following, we derive an approximate expression for the PDF of $\gamma_{\rm up}$. We start by determining the CDF of $\gamma_{\rm up}$

$$\begin{aligned}
F_{\gamma_{\rm up}}(x)&=\mathbb{P}(\gamma_{\rm up}\leq x)=1-\mathbb{P}(\gamma_{\rm up}\geq x)\\
&=1-\mathbb{P}(\min(\gamma_{{\rm eq}\,1},\ldots,\gamma_{{\rm eq}\,N})\geq x)\\
&=1-\prod_{n=1}^{N}\mathbb{P}(\gamma_{{\rm eq}\,n}\geq x)=1-\prod_{n=1}^{N}(1-F_{\gamma_{{\rm eq}\,n}}(x))\\
&=\sum_{n=1}^{N}F_{\gamma_{{\rm eq}\,n}}(x)-\sum_{n,n'}F_{\gamma_{{\rm eq}\,n}}(x)F_{\gamma_{{\rm eq}\,n'}}(x)\\
&\quad+\ldots+(-1)^{N+1}\prod_{n=1}^{N}F_{\gamma_{{\rm eq}\,n}}(x)\underset{\rm SIR\gg 1}{\approx}\sum_{n=1}^{N}F_{\gamma_{{\rm eq}\,n}}(x).
\end{aligned}\tag{52}$$

At high SIR, the terms of the first order are dominant which explain the approximation in (52). Taking the derivative of CDF $F_{\gamma_{\text{up}}}(x)$ with respect to x, we can determine an approximate expression for the PDF $f_{\gamma_{\text{up}}}(x)$ as

$$f_{\gamma_{\text{up}}}(x) \approx \sum_{n=1}^{N} f_{\gamma_{\text{eq n}}}(x). \tag{53}$$

Using a similar procedure as in [28, Appendix I], the PDF of $f_{\gamma_{\text{eq n}}}(x)$ is determined as

$$f_{\gamma_{\text{eq n}}}(x) = \frac{x^{\alpha_n - 1}}{w_n^{\alpha_n} B(\alpha_n, A_n)} \left(1 + \frac{x}{w_n}\right)^{-B_n}. \tag{54}$$

Utilizing (50) and (53), we approximate the BEP as

$$\begin{aligned} P_e &\approx \int_0^{\infty} P_{e|\gamma_{\text{up}}} f_{\gamma_{\text{up}}}(x)\, dx = \int_0^{\infty} a \exp(-bx) f_{\gamma_{\text{up}}}(x)\, dx \\ &\approx \int_0^{\infty} a \exp(-bx) \left(\sum_{n=1}^{N} f_{\gamma_{\text{eq n}}}(x)\right) dx. \end{aligned} \tag{55}$$

In (55), the first term in the integral has its maximum at $x = 0$. This term is monotonically decreasing and decays very fast to null as x increases. The behaviour of the PDFs $f_{\gamma_{\text{eq n}}}(x)$ around $x = 0$ has more impact in the evaluation of the integral in (55) [29], [30]. Using the series expansion of $(1 + x)^{\alpha}$ as $x \to 0$ and utilizing (54), we can approximate the PDFs $f_{\gamma_{\text{eq n}}}(x)$ as

$$f_{\gamma_{\text{eq n}}}(x) \approx \frac{x^{\alpha_n - 1}}{w_n^{\alpha_n} B(\alpha_n, A_n)}. \tag{56}$$

It follows that the BEP at high SIR is approximated as

$$\begin{aligned} P_e &\approx \int_0^{\infty} a \exp(-bx) \left(\sum_{n=1}^{N} \frac{x^{\alpha_n - 1}}{w_n^{\alpha_n} B(\alpha_n, A_n)}\right) dx \\ &= \sum_{n=1}^{N} \frac{a b^{-\alpha_n} \Gamma(\alpha_n)}{w_n^{\alpha_n} B(\alpha_n, A_n)} = \sum_{n=1}^{N} \frac{a b^{-\alpha_n} \Gamma(\alpha_n) \alpha_n^{\alpha_n}}{\mathsf{SIR}_n^{\alpha_n} A_n^{\alpha_n} B(\alpha_n, A_n)}. \end{aligned} \tag{57}$$

In (57), we used the relationship $w_n = \mathsf{SIR}_n A_n / \alpha_n$, where SIR_n stands for the average SIR at the nth hop. From (57), it can be deduced that the BEP of the system can be reduced by increasing the SIR at all the links of the multihop relay network. If only one single hop has a low SIR, this will degrade the whole system BEP performance. Numerical results in Section IX show that the approximation in (57) is very tight at high SIR. Therefore, using the expression in (57) both the diversity gain d_g and the coding gain c_g of the system are deduced as

$$d_g = \alpha_m = \min\{\alpha_1, \ldots, \alpha_N\} \tag{58}$$

$$c_g = \frac{a b^{-\alpha_m} \Gamma(\alpha_m) \alpha_m^{\alpha_m}}{A_m^{\alpha_m} B(\alpha_m, A_m)}, \tag{59}$$

where m is the subscript of $\alpha_m = \min\{\alpha_1, \ldots, \alpha_N\}$. This implies that the BEP performance is governed by the hop that has the worst propagation condition for the desired signal which is the hop with the smallest value of α_n. We can conclude from (58) that at high SIR regime the slope of the BEP is given by α_m, whereas the number of interferers at this hop has no impact on the slope of the BEP.

It has to be noted that at high SIR regime the lower-bound of the BEP provided by (49) has the same slope as the exact BEP in (25). In other words, the diversity order of the lower-bound in (49) is equal to α_m.

Proof: See Appendix B. ∎

VIII. SYSTEM OPTIMIZATION

In this section, we aim to determine the optimal power allocation at the source device and the relay devices $R_n\,(n = 1, \ldots, N-1)$ such that the BEP is minimized. This optimization is performed subject to a sum power constraint. The total power P_T is equal to the sum of the power P_0 assigned to the source device and the powers $P_n\,(n = 1, \ldots, N-1)$ assigned to the relays R_n, i.e., $P_T = \sum_{n=1}^{N} P_{n-1}$. We consider that the transmitters have knowledge about the channel statistics. More specifically, the source device knows the average power $\mathbb{E}(h_1^2)$ of the channel between the source and the relay R_1. Similarly, the relay R_{n-1} knows the value of the average power $\mathbb{E}(h_n^2)$ of the channel between the relays R_{n-1} and R_n. The optimization problem is formulated as follows

$$\begin{aligned} &\underset{P_0, \ldots, P_{n-1}, \ldots, P_{N-1}}{\text{minimize}} \quad P_e \\ &\text{subject to} \sum_{n=1}^{N} P_{n-1} = P_T \\ &\qquad P_0, \ldots, P_{n-1}, \ldots, P_{N-1} > 0. \end{aligned} \tag{60}$$

To solve this optimization problem, we need first to express the error probability P_e in (57) in terms of the powers $P_0, \ldots, P_{n-1}, \ldots, P_{N-1}$. To this end, we express the average SIR of the nth hop as follows

$$\mathsf{SIR}_n = \frac{\bar{\gamma}_n}{\bar{\gamma}_{In}} = \frac{P_{n-1} \mathbb{E}(h_n^2)}{\bar{\gamma}_{In}}. \tag{61}$$

Using (57), (61), and (8), the BEP P_e can now be expressed as

$$P_e = \sum_{n=1}^{N} \frac{C_n}{(P_{n-1})^{\alpha_n}}, \tag{62}$$

where

$$C_n = \frac{a\, b^{-\alpha_n} \Gamma(\alpha_n) \alpha_n^{\alpha_n} \bar{\gamma}_{In}^{\alpha_n} (4\pi d_0)^{2\alpha_n} d_n^{\eta\alpha_n}}{\lambda^{2\alpha_n} d_0^{\eta\alpha_n} A_n^{\alpha_n} B(\alpha_n, A_n)}. \tag{63}$$

The optimization problem in (60) is rewritten using (62) as

$$\begin{aligned} &\underset{P_0, \ldots, P_{n-1}, \ldots, P_{N-1}}{\text{minimize}} \quad P_e = \sum_{n=1}^{N} \frac{C_n}{(P_{n-1})^{\alpha_n}} \\ &\text{subject to} \sum_{n=1}^{N} P_{n-1} = P_T \\ &\qquad P_0, \ldots, P_{n-1}, \ldots, P_{N-1} > 0. \end{aligned} \tag{64}$$

Next, we first prove that the optimal solution that minimize the BEP is unique and then provide an exact expression for the optimal powers $P_0^*, \ldots, P_{n-1}^*, \ldots, P_{N-1}^*$. To prove

the uniqueness of the solution, we have to show that the optimization problem in (64) is convex. We recall that for an optimization problem to be convex, the objective function should be convex, the equality constraints should be linear, and the inequality constraints should be convex [31]. For our optimization problem (64), both the equality and the inequality constraints are linear. Thus, to show that the optimization problem in (64) is convex, it suffices to prove that the objective function is convex. Towards this end, we will use the fact that the sum of convex functions is a convex function [31]. Since the objective function in (64) is a sum of N functions, we need to show that each of these functions is convex. By computing the second derivative of each terms, we obtain

$$\frac{\partial^2 \left(C_n \left(P_{n-1}\right)^{-\alpha_n}\right)}{\partial P_{n-1}^2} = C_n \alpha_n (\alpha_n + 1) \left(P_{n-1}\right)^{-\alpha_n - 2}. \quad (65)$$

Since $C_n \geq 0$ and the severity of fading parameter $\alpha_n \geq 1/2$, then $\left(C_n \left(P_{n-1}\right)^{-\alpha_n}\right)$ is convex for $n = 1, \ldots, N$. Consequently, the objective function in (64) is convex and the optimization problem in (64) has a unique solution.

In the following, we determine the optimal values of the powers $P_0^*, \ldots, P_{n-1}^*, \ldots, P_{N-1}^*$ which minimize the BEP. First, we write the Lagrangian of (64) as

$$\mathcal{L}(P_0, \ldots, P_{N-1}, \lambda, \kappa_0, \ldots, \kappa_{N-1}) = \sum_{n=1}^{N} \frac{C_n}{(P_{n-1})^{\alpha_n}} + \lambda \left(\sum_{n=1}^{N} P_{n-1} - P_T \right) - \sum_{n=1}^{N} \kappa_{n-1} P_{n-1}, \quad (66)$$

where $\lambda, \kappa_0, \ldots, \kappa_{N-1}$ are the Lagrangian coefficients. Using the fact that the Karush–Khun–Tucker conditions are necessary for an optimal solution, we obtain

$$\left. \frac{\partial \mathcal{L}}{\partial P_{n-1}} \right|_{(P_0^*, \ldots, P_{N-1}^*, \lambda^*, \kappa_0^*, \ldots, \kappa_{N-1}^*)} = 0 \quad \text{for } 1 \leq n \leq N \quad (67)$$

$$\sum_{n=1}^{N} P_{n-1}^* - P_T = 0 \quad (68)$$

$$\kappa_{n-1}^* P_{n-1}^* = 0 \quad \text{for } 1 \leq n \leq N. \quad (69)$$

Since the objective is to minimize the BEP $\sum_{n=1}^{N} C_n / \left(P_{n-1}\right)^{\alpha_n}$, we can deduce from (69) that $\kappa_{n-1}^* = 0$ $(n = 1, \ldots, N)$ since the power allocated to each node is strictly positive, i.e. $P_{n-1}^* > 0$ for $n = 1, \ldots, N$. Using (67), we get

$$\lambda^* = \frac{\alpha_n C_n}{\left(P_{n-1}^*\right)^{\alpha_n + 1}} \quad \forall n = 1, \ldots, N. \quad (70)$$

Utilizing (70), we can find a relation between the optimal powers at each hop as

$$\frac{\alpha_1 C_1}{\left(P_0^*\right)^{\alpha_1 + 1}} = \frac{\alpha_n C_n}{\left(P_{n-1}^*\right)^{\alpha_n + 1}} \quad \forall n = 2, \ldots, N \quad (71)$$

$$P_{n-1}^* = \left[\frac{\alpha_n C_n}{\alpha_1 C_1} \right]^{1/(\alpha_n + 1)} \left(P_0^*\right)^{(\alpha_1 + 1)/(\alpha_n + 1)} = \Lambda_n \left(P_0^*\right)^{(\alpha_1 + 1)/(\alpha_n + 1)} \quad \forall n = 2, \ldots, N. \quad (72)$$

Using (68) and (72), we find a relation between P_0^* and the total power P_T as

$$\sum_{n=1}^{N} P_{n-1}^* = P_0^* + \sum_{n=2}^{N} \Lambda_n \left(P_0^*\right)^{(\alpha_1 + 1)/(\alpha_n + 1)} = P_T. \quad (73)$$

The optimal power P_0^* is determined by solving (73) numerically using standard root-finding algorithms such as gradient descent and Newton's method. After determining P_0^*, the optimal power P_{n-1}^* is computed using (72). Note that if the severity of fading for all the hops is the same, i.e., $\alpha_1 = \ldots = \alpha_n \ldots = \alpha_N = \alpha$, a closed-from expression for the optimal power P_0^* is obtained as

$$P_0^* = \frac{P_T}{1 + \sum_{n=2}^{N} \Lambda_n'}, \quad (74)$$

where

$$\Lambda_n' = \left[C_n / C_1\right]^{1/(\alpha+1)} = \left[\frac{\bar{\gamma}_{In}^{\alpha} d_n^{\eta\alpha} A_1^{\alpha} B(\alpha, A_1)}{\bar{\gamma}_{I1}^{\alpha} d_1^{\eta\alpha} A_n^{\alpha} B(\alpha, A_n)} \right]^{1/(\alpha+1)}. \quad (75)$$

The expression of the optimal power P_{n-1}^* is obtained as

$$P_{n-1}^* = \Lambda_n' P_0^* = \frac{\Lambda_n' P_T}{1 + \sum_{i=2}^{N} \Lambda_i'}. \quad (76)$$

The optimal power strategy attempts to improve the quality of the links that suffer from the worst communication conditions by allocating more power to these worst links. This strategy allows maintaining a balance between the SIR levels in different hops, which minimizes the BEP. As discussed in Section VII, if the SIR drops for a single hop, the whole system performance degrades. To avoid such situation, the power at different nodes should be allocated according to (76) which minimizes the BEP. From (76), it can be deduced that the optimal power P_{n-1}^* at the relay R_{n-1} increases if Λ_n' increases. Using the expression of Λ_n' in (75), it can be concluded that Λ_n' increases if: (i) the interference level $\bar{\gamma}_{In}$ affecting the nth relay is larger than the interference level $\bar{\gamma}_{I1}$ affecting the first relay, or (ii) the power attenuation due to the distance travelled by the signal is larger for the nth hop compared to the first hop.[2] In these cases, the power P_{n-1}^* allocated to the relay R_{n-1} should be larger than the power P_0^* allocated to the source device.

IX. NUMERICAL RESULTS

In this section, the analytical results presented in the previous section are evaluated numerically and illustrated. First, the expression of the PDF of the product of the rational power of the ratio of Gamma RVs is validated by Monte Carlo simulations. Then we provide the results for the exact BEP together with its corresponding lower-bound to check the tightness of the proposed bound as well as the effect of the number of hops on the performance. Finally, the effect of

[2]Note that the power attenuation due to the travelled distance increases proportionally with the distance between communicating devices. This implies that if the distance d_n between the relay R_{n-1} and the relay R_n is larger than the distance between the source device and the first relay R_1, Λ_n' and P_{n-1}^* increase, i.e. more power should be allocated to the relay R_{n-1}.

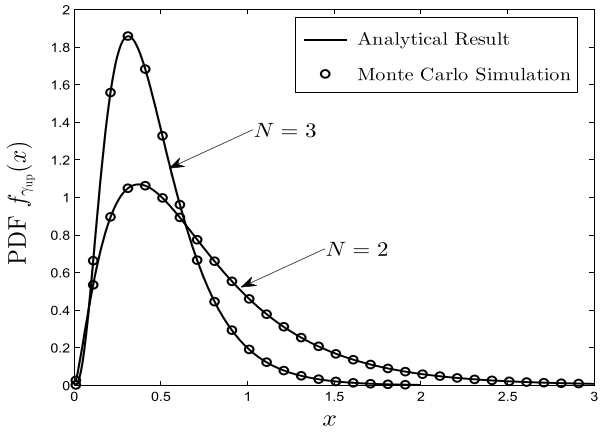

FIGURE 2. Comparison between the analytical results (44) and the Monte Carlo simulation for the PDF of the upper-bound γ_{up} for two and three multihop scenarios.

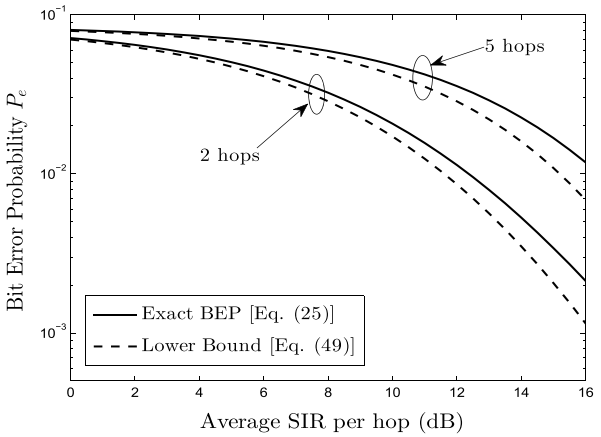

FIGURE 3. Exact and lower-bound results for the BEP of 16-QAM modulation scheme over an AF multihop system over Nakagami-*m* channels.

the number of interferes on the BEP performance is illustrated and discussed.

In Fig. 2, we illustrate the PDF of the SIR upper-bound γ_{up}. From this figure, it can be seen that a good match is obtained between the analytical expression of the PDF presented in (44) and the Monte Carlo simulations.[3] This facts confirms the validity of the analytical expression of the PDF in (44) as well as the correctness of Corollary 1. In Fig. 2, we depict the PDF of γ_{up} for two different scenarios. In the first scenario, we have a two-hop relay network with both the relay node and the destination node affected by three interferes each, i.e., $L_1 = L_2 = 3$. The fading channel of the interferes affecting the relay and the destination have a severity of fading $a_1 = 3.1$ and $a_2 = 2.3$, respectively. The fading channel experienced by the desired signal have a severity of fading $\alpha_1 = 1.5$ and $\alpha_2 = 1.3$ for the first and the second hop, respectively. In the second scenario, we add a second relay and have in total there hops with parameters $\alpha_1 = 1.5$, $\alpha_2 = 1.3$, and $\alpha_3 = 2$. The number of interferes in the second scenario is set to $L_1 = L_2 = L_3 = 3$. The severity of fading for the interference links is $a_1 = 3.1$, $a_2 = 2.3$, and $a_3 = 2$.

In Fig. 3, we depict both the exact result and the lower-bound for the BEP for the case of 16-QAM modulation scheme. The lower-bound expression is given by (49) whereas for the curve of the exact result is obtained through Monte Carlo simulation. The exact analytical expression for the BEP is given by (25) in terms of the multivariate Meijer's G-function. This function is evaluated numerically in MATHEMATICA. In Fig. 3, we illustrate the impact of the number of hops on the system performance. A two-hop and a five-hop relay networks are considered. In our simulation, the desired signal undergoes identically distributed fading channels in all the links and the value of $\alpha_n = 2.5$ for all the hops. Note that the expression of the exact BEP in (25) is valid for both cases of identically and non-identically distributed fading channels. The number of interferes is equal to 3 at each node, i.e., $L_n = 3$. The severity of fading on the interference link is set to $a_n = 2.7$. From Fig. 3, it can be noticed that the error probability deteriorates as the number of hops in the system increases. Moreover, the proposed bound is quite tight at low and medium SIR region. The tightness of the lower-bound decays for high SIR regime but remains within an acceptable range.

We notice as well from the trend of the curves at high SIR that the slope of the BEP is not affected by the number of hops. This fact is confirmed by (58) from which it can be concluded that the slope of the BEP at high SIR is not affected by the number of hops N but depends only on the minimum value $\alpha_m = \min(\alpha_1, \ldots, \alpha_N)$. Since for both the two-hop and the five-hop scenarios, we kept the value of α_n unchanged, it is natural that we obtain the same slope of the BEP curves at high SIR even if the number of hops varies. It has to be noted that at high SIR regime the BEP lower-bound in (49) has the same slope as the exact BEP in (25). This fact is proven in Appendix B where we show that the BEP lower-bound has the same diversity order of the exact BEP, which is equal to α_m.

In Fig. 4, we illustrate the impact of the number of interferers on the BEP. In the considered scenario, we have a three-hop relay network with i.i.d. fading channels on each hop and we set the value of α_n to 1.5. The number of interferers at each node is kept the same in each of the curves illustrated in Fig. 4, while the severity of fading for the interference link is set to $a_n = 1.2$. The BEP results shown in this figure are obtained for the case of a BPSK modulation scheme. We set the transmission power P_n at each node to a constant value P_0 and consider the case where the interferers have equal power, i.e., $P_{In,i} = P$ [see (5)]. We denote by ζ the ratio of P_0 and P, i.e., $\zeta = P_0/P$. Note that ζ is different from the SIR per hop. Numerical results, which are not presented here, showed that if the SIR per hop is kept the same, the number

[3]The results for the Monte Carlo simulations are obtained by using 100 million samples.

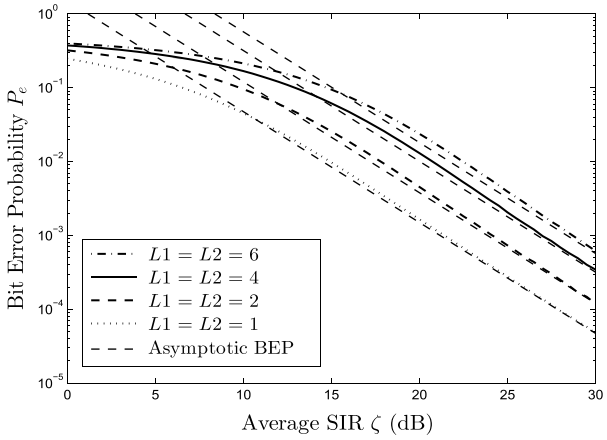

FIGURE 4. The impact of the number of interferes on the BEP over a 3 hops AF relaying system.

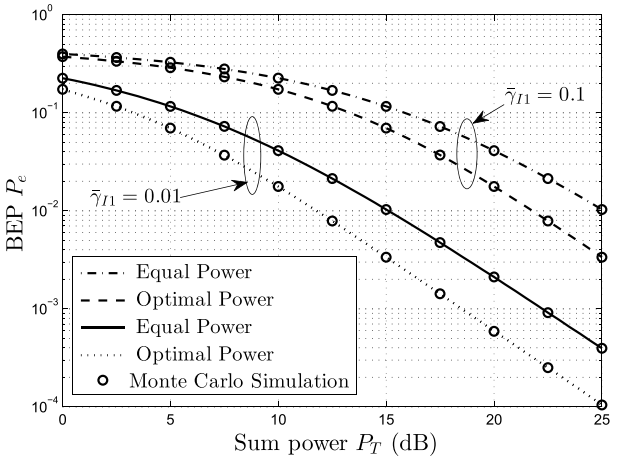

FIGURE 5. BEP performance with optimized and equal power allocation for a three-hop network.

of interferes would have almost no impact on the BEP. Therefore, we illustrate instead the BEP versus the SIR ζ in Fig. 4. From this figure, we can conclude that the BEP decreases as ζ increases. Moreover, for a fixed value of ζ the BEP decreases as the number of interferers decreases. Note that since each of the interferes have equal power then the increase of number of interferers results in the drop of the total SIR and consequently the BEP performance deteriorate as the number of interferers L_n increases. For all the curves in Fig. 4, it can be noticed that the slope at high SIR is the same. This is due to the fact that the parameters $\alpha_n (n = 1, \ldots, N)$ are kept the same for all the curves in Fig. 4. Actually, it can be deduced from (58) that the slope of the BEP at high SIR depends only on the parameter $\alpha_m = \min(\alpha_1, \ldots, \alpha_N)$ and is not affected by the number of interferers L_n. In Fig. 4, we plot as well the asymptotic result for the BEP given by (57). At high SIR, a good match is obtained between the exact and the asymptotic results for the BEP. This justifies the use of the asymptotic BEP in (57) to determine both the diversity order and the coding gain of the system.

In Fig. 5, we depict the BEP versus the sum power P_T for the cases of equal and optimal power allocations. We consider in the investigated scenario a three-hop network composed of a source device, destination device and two relay devices. For the optimal power allocation scheme, the total power P_T is split between the different devices (the source and the relays) according to (76). In the investigated scenario, the mean power of the interference $\bar{\gamma}_{I1}$ affecting the relay R_1 is set to 0.1 and 0.01. Whereas the interference mean powers affecting the relay R_2 and the destination node D are equal to $\bar{\gamma}_{I2} = \bar{\gamma}_{I1}$ and $\bar{\gamma}_{I3} = 100\bar{\gamma}_{I1}$, respectively. Thus, the third hop suffers from higher interference compared to the first and the second hop. In order to minimize the BEP, a much larger power should be allocated to the relay R_2. From Fig. 5, it can be observed that the BEP decreases by using optimal power allocation compared to the equal power allocation scheme. The gain achieved thanks to optimal power allocation compared to the equal power allocation is equal to 3.5 dB if we have a target BEP of 10^{-2} and for $\bar{\gamma}_{I1} = 0.1$. For a target BEP of 10^{-3} and $\bar{\gamma}_{I1} = 0.01$, the optimal power allocation strategy allows achieving a gain of 3.8 dB compared to the equal power allocation scheme. It can be seen from Fig. 5 that the BEP decays as the interference decays. In Fig. 5, a perfect match is obtained between the numerical expressions and the Monte Carlo simulations which proves the validity of the our results.

X. CONCLUSION

This paper investigated the BEP of mmWave AF multihop relaying systems in presence of external interference. In a first step, we derive the exact expression of the average BEP of the multihop relay system for M-QAM and M-PSK in terms of multivariate Meijer's G-function. This latter function is complicated and does not allow getting a clear insight on the behaviour of the BEP. Therefore, it was required to derive a bound for the BEP of mmWave multihop relaying systems. To this aim, we determined an upper-bound for the end-to-end SIR as a product of the rational power of the ratio of Gamma RVs. Using a novel Mellin-approach, we derived closed-form expressions for the statistics of the SIR upper-bound, such as the Mellin transform, the PDF, the CDF, and the MGF. The correctness of the PDF expression has been validated by Monte Carlo simulations. Utilizing the PDF of the SIR upper-bound, a lower-bound for the BEP of M-QAM and M-PSK modulation schemes in multihop AF relaying systems in presence of interference have been determined. This lower-bound is expressed in terms of a Meijer's G-function. A simple asymptotic expression for the BEP is also derived which allowed getting a clear insight of the effect of the different system parameters on the BEP performance.

Numerical results have shown that the tightness of the proposed BEP lower-bound especially at low SIR. Our analysis revealed that the BEP performance deteriorates if the number of hops increases. If we assume equal SIR per hop, the BEP performance is mainly governed by the hop with the worst

propagation condition for the desired signal. If the number of interferers is increased while keeping the same level of SIR per hop unchanged, almost no variation in the BEP is observed. However, if the interference level increases with the number of interferers added while keeping the fading channel for the desired signal unchanged, the BEP deteriorates but the slope of the BEP at high SIR regime remains the same.

Moreover, we formulated the problem of BEP minimization of multihop mmWave relay network subject to a sum power constraint. We showed that this problem admits a unique solution and derived analytical expression for the optimal power allocation at each hop. Our numerical study revealed that the optimal power allocation allows achieving more than 3 dB gain compared to the equal power allocation scheme. A perfect match between our analytical results and Monte Carlo simulations proves the validity of our results.

APPENDIX A
PROOF OF THEOREM 1

In this appendix, we provide the proof for the Mellin transform of the product of rational powers of ratio of Gamma RVs. The RV Z is given by

$$Z = \prod_{n=1}^{N} \left(\frac{X_n}{Y_n}\right)^{1/N} = \prod_{n=1}^{N} (U_n)^{1/N} = \prod_{n=1}^{N} V_n \quad \text{(A.1)}$$

Using Lemma 3 and Lemma 2, we can derive the Mellin transform of Z as

$$\mathcal{M}_s(Z) = \prod_{n=1}^{N} \mathcal{M}_s(V_n) = \prod_{n=1}^{N} \mathcal{M}_{\frac{1}{N}s-\frac{1}{N}+1}(U_n). \quad \text{(A.2)}$$

Since U_n is the ratio of two independent positive RVs $U_n = \frac{X_n}{Y_n}$, we can evaluate the Mellin transform of U_n using Lemma 4 as

$$\mathcal{M}_t(U_n) = \mathcal{M}_t(X_n)\mathcal{M}_{2-t}(Y_n). \quad \text{(A.3)}$$

In the following, we determine the Mellin transforms $\mathcal{M}_t(X_n)$ and $\mathcal{M}_{2-t}(Y_n)$. The Mellin transform $\mathcal{M}_t(X_n)$ is computed as

$$\begin{aligned}\mathcal{M}_t(X_n) &= \int_0^\infty x^{t-1} f_{X_n}(x)dx \\ &= \int_0^\infty x^{t-1} \frac{x^{\alpha_n-1}}{\beta_n^{\alpha_n}\Gamma(\alpha_n)} \exp\left(-\frac{x}{\beta_n}\right) dx \\ &= \left(\frac{1}{\beta_n}\right)^{1-t} \frac{\Gamma(\alpha_n-1+t)}{\Gamma(\alpha_n)}. \end{aligned} \quad \text{(A.4)}$$

As Y_n is Gamma distributed, its Mellin transform $\mathcal{M}_t(Y_n)$ has a similar expression to $\mathcal{M}_t(X_n)$. The Mellin transform $\mathcal{M}_t(Y_n)$ can obtained as

$$\mathcal{M}_s(Y_n) = \left(\frac{1}{b_n}\right)^{1-s} \frac{\Gamma(a_n-1+s)}{\Gamma(a_n)}. \quad \text{(A.5)}$$

The expression of $\mathcal{M}_{2-t}(Y_n)$ is deduced from (A.5) by setting s to $2-t$ as

$$\mathcal{M}_{2-t}(Y_n) = \mathcal{M}_s(Y_n)\Big|_{s=2-t} = \left(\frac{1}{b_n}\right)^{t-1} \frac{\Gamma(a_n+1-t)}{\Gamma(a_n)}. \quad \text{(A.6)}$$

Utilizing (A.3), (A.4), and (A.6), the Mellin Transform $\mathcal{M}_t(U_n)$ is determined as

$$\begin{aligned}\mathcal{M}_t(U_n) &= \mathcal{M}_t(X_n)\mathcal{M}_{2-t}(Y_n) \\ &= \left(\frac{b_n}{\beta_n}\right)^{1-t} \frac{\Gamma(\alpha_n-1+t)}{\Gamma(\alpha_n)} \frac{\Gamma(a_n+1-t)}{\Gamma(a_n)}. \end{aligned} \quad \text{(A.7)}$$

To obtain the expression of $\mathcal{M}_s(Z)$, we need first to compute $\mathcal{M}_{\frac{1}{N}s-\frac{1}{N}+1}(U_n)$ which is deduced from $\mathcal{M}_t(U_n)$ as

$$\begin{aligned}\mathcal{M}_{\frac{1}{N}s-\frac{1}{N}+1}(U_n) &= \mathcal{M}_t(U_n)\Big|_{t=\frac{1}{N}s-\frac{1}{N}+1} \\ &= \left(\frac{b_n}{\beta_n}\right)^{(1-s)/N} \frac{\Gamma(\alpha_n+(s-1)/N)}{\Gamma(\alpha_n)} \\ &\quad \times \frac{\Gamma(a_n+(1-s)/N)}{\Gamma(a_n)}. \end{aligned} \quad \text{(A.8)}$$

Using (A.2) and (A.8), the Mellin Transform of Z is determined as in (34).

APPENDIX B
DIVERSITY ORDER OF (49)

In this appendix, we show that the diversity order of the lower-bound of the BEP in (49) has a diversity order equal to $\alpha_m = \min\{\alpha_1, \ldots, \alpha_N\}$. Towards this end, we rewrite the lower-bound in (49) as

$$P_{e,\text{low}} = C \cdot G_{2N,N}^{N,2N}\left(z\middle|\begin{matrix}\mathbf{A}\\ \mathbf{B}\end{matrix}\right), \quad \text{(B.1)}$$

where $C = \frac{a}{\left(\sqrt{2\pi}\right)^{N-1}\sqrt{N}\prod_{n=1}^{N}\Gamma(\alpha_n)\Gamma(L_n a_n)}$, $\mathbf{A} = \Psi(1-L_n a_n), \Theta\left(\frac{k}{N}\right)$ and $\mathbf{B} = \alpha_1, \ldots, \alpha_n, \ldots, \alpha_N$. Note that $\mathbf{A}$ comprises $2N$ elements, while $\mathbf{B}$ comprises N elements. The argument z of the Meijer's G-function in (B.1) is expressed in terms of the average SIR at the nth hop SIR_n as

$$z = \left(\prod_{n=1}^{N}\left(\frac{b_n}{\beta_n}\right)\right)\left(\frac{N}{b}\right)^N = \prod_{n=1}^{N}\left(\frac{N\alpha_n}{bL_n a_n \mathsf{SIR}_n}\right). \quad \text{(B.2)}$$

In (B.2), we used the relationship between the SIR at the nth hop, SIR_n, and the parameters b_n and β_n which is given by $\frac{b_n}{\beta_n} = \frac{\alpha_n}{L_n a_n \mathsf{SIR}_n}$. Note that at high SIR regime $\mathsf{SIR}_n \to \infty$ for $n = 1, \ldots, N$ and consequently the term z in (B.2) tends to zero.

Using the relationship between the H-Fox function and the Meijer's G-function in [32, eq. (2.9.1)] as well as the asymptomatic expression for the H-Fox function in [32, Corollary 1.11.1], we obtain an asymptotic expression for the lower-bound of the BEP in (B.1) at high SIR regime as

$$\begin{aligned}\lim_{\mathsf{SIR}\to\infty} P_{e,\text{low}} &= \lim_{z\to 0} C \cdot G_{2N,N}^{N,2N}\left(z\middle|\begin{matrix}\mathbf{A}\\ \mathbf{B}\end{matrix}\right) \\ &= Ce_m z^{\alpha_m} + o(z^{\alpha_m}), \end{aligned} \quad \text{(B.3)}$$

where

$$e_m = \prod_{\substack{i=1\\ i\neq m}}^{N}\Gamma(\alpha_i-\alpha_m)\prod_{i=1}^{N}\Gamma(L_i a_i+\alpha_m)\prod_{k=0}^{N-1}\Gamma\left(\frac{k}{N}+\alpha_m\right) \quad \text{(B.4)}$$

and $o(\cdot)$ pertains to the Landau notation defined as $\lim_{z\to 0} |o(z)/z| = 0$. From (B.3), it can be deduced that the diversity order of the lower-bound $P_{e,\text{low}}$ is equal to α_m, thus both the exact BEP in (25) and its lower-bound $P_{e,\text{low}}$ in (49) have the same slope at high SIR regime.

ACKNOWLEDGMENT

This work was carried out during the tenure of an ERCIM "Alain Bensoussan" Fellowship Programme.

REFERENCES

[1] "Cisco visual networking index: Forecast and methodology, 2015–2020," Cisco, San Jose, CA, USA, White Paper, Jun. 2016.
[2] Z. Pi and F. Khan, "An introduction to millimeter-wave mobile broadband systems," *IEEE Commun. Mag.*, vol. 49, no. 6, pp. 101–107, Jun. 2011.
[3] T. S. Rappaport *et al.*, "Millimeter wave mobile communications for 5G cellular: It will work!" *IEEE Access*, vol. 1, pp. 335–349, May 2013.
[4] S. Akoum, O. El Ayach, and R. W. Heath, Jr., "Coverage and capacity in mmWave cellular systems," in *Proc. Conf. Rec. 46th Asilomar Conf. Signals, Syst. Comput. (ASILOMAR)*, Nov. 2012, pp. 688–692.
[5] F. Khan and Z. Pi, "mmWave mobile broadband (MMB): Unleashing the 3–300 GHz spectrum," in *Proc. 34th IEEE Sarnoff Symp.*, May 2011, pp. 1–6.
[6] M. K. Samimi *et al.*, "28 GHz angle of arrival and angle of departure analysis for outdoor cellular communications using steerable beam antennas in New York City," in *Proc. IEEE 77th Veh. Technol. Conf. (VTC Spring)*, Jun. 2013, pp. 1–6.
[7] S. Nie, G. R. MacCartney, Jr., S. Sun, and T. S. Rappaport, "72 GHz millimeter wave indoor measurements for wireless and backhaul communications," in *Proc. IEEE 24th Annu. Int. Symp. Pers., Indoor, Mobile Radio Commun. (PIMRC)*, Sep. 2013, pp. 2429–2433.
[8] S. Singh, F. Ziliotto, U. Madhow, E. Belding, and M. Rodwell, "Blockage and directivity in 60 GHz wireless personal area networks: From cross-layer model to multihop MAC design," *IEEE J. Sel. Areas Commun.*, vol. 27, no. 8, pp. 1400–1413, Oct. 2009.
[9] J. Qiao, L. X. Cai, X. S. Shen, and J. W. Mark, "Enabling multi-hop concurrent transmissions in 60 GHz wireless personal area networks," *IEEE Trans. Wireless Commun.*, vol. 10, no. 11, pp. 3824–3833, Nov. 2011.
[10] J. Kim and A. F. Molisch, "Quality-aware millimeter-wave device-to-device multi-hop routing for 5G cellular networks," in *Proc. IEEE Int. Conf. Commun. (ICC)*, Jun. 2014, pp. 5251–5256.
[11] N. Eshraghi, B. Maham, and V. Shah-Mansouri, "Millimeter-wave device-to-device multi-hop routing for multimedia applications," in *Proc. IEEE Int. Conf. Commun. (ICC)*, May 2016, pp. 1–6.
[12] X. Lin and J. G. Andrews, "Connectivity of millimeter wave networks with multi-hop relaying," *IEEE Wireless Commun. Lett.*, vol. 4, no. 2, pp. 209–212, Apr. 2015.
[13] T. Bai, A. Alkhateeb, and R. W. Heath, Jr., "Coverage and capacity of millimeter-wave cellular networks," *IEEE Commun. Mag.*, vol. 52, no. 9, pp. 70–77, Sep. 2014.
[14] T. Bai and R. W. Heath, Jr., "Coverage and rate analysis for millimeter-wave cellular networks," *IEEE Trans. Wireless Commun.*, vol. 14, no. 2, pp. 1100–1114, Feb. 2015.
[15] M. O. Hasna and M. S. Alouini, "Outage probability of multihop transmission over Nakagami fading channels," *IEEE Commun. Lett.*, vol. 7, no. 5, pp. 216–218, May 2003.
[16] I. S. Gradshteyn and I. M. Ryzhik, *Table of Integrals, Series, and Products*, 7th ed. San Francisco, CA, USA: Academic, 2007.
[17] Y. Azar *et al.*, "28 GHz propagation measurements for outdoor cellular communications using steerable beam antennas in New York city," in *Proc. IEEE Int. Conf. Commun. (ICC)*, Jun. 2013, pp. 5143–5147.
[18] T. S. Rappaport, F. Gutierrez, Jr., E. Ben-Dor, J. N. Murdock, Y. Qiao, and J. I. Tamir, "Broadband millimeter-wave propagation measurements and models using adaptive-beam antennas for outdoor urban cellular communications," *IEEE Trans. Antennas Propag.*, vol. 61, no. 4, pp. 1850–1859, Apr. 2013.
[19] K. J. Hole, H. Holm, and G. E. Oien, "Adaptive multidimensional coded modulation over flat fading channels," *IEEE J. Sel. Areas Commun.*, vol. 18, no. 7, pp. 1153–1158, Jul. 2000.
[20] T. Soithong, V. A. Aalo, G. P. Efthymoglou, and C. Chayawan, "Outage analysis of multihop relay systems in interference-limited Nakagami-*m* fading channels," *IEEE Trans. Veh. Technol.*, vol. 61, no. 3, pp. 1451–1457, Mar. 2012.
[21] *Mathematica Edition: Version 8.0.*, Wolfram Res., Champaign, IL, USA, 2010.
[22] H. M. Srivastava and R. Panda, "Expansion theorems for the H function of several complex variables," *J. Reine Angew. Math.*, vol. 1976, no. 288, pp. 129–145, 1976.
[23] I. S. Ansari, S. Al-Ahmadi, F. Yilmaz, M.-S. Alouini, and H. Yanikomeroglu, "A new formula for the BER of binary modulations with dual-branch selection over generalized-*K* composite fading channels," *IEEE Trans. Commun.*, vol. 59, no. 10, pp. 2654–2658, Oct. 2011.
[24] H. M. Srivastava and R. G. Buschman, *Theory and Applications of Convolution Integral Equations*. Dordrecht, The Netherlands: Kluwer, 1992.
[25] A. P. Prudnikov, Y. A. Brychkov, and O. I. Marichev, *Integrals and Series: Direct Laplace Transforms*, vol. 4, 1st ed. Boca Raton, FL, USA: CRC Press, 1992.
[26] M. Abramowitz and I. A. Stegun, *Handbook of Mathematical Functions: With Formulas, Graphs, and Mathematical Tables*. New York, NY, USA: Dover, 1964.
[27] G. K. Karagiannidis, T. A. Tsiftsis, and R. K. Mallik, "Bounds for multihop relayed communications in Nakagami-*m* fading," *IEEE Trans. Commun.*, vol. 54, no. 1, pp. 18–22, Jan. 2006.
[28] A. Ghasemi and E. S. Sousa, "Fundamental limits of spectrum-sharing in fading environments," *IEEE Trans. Wireless Commun.*, vol. 6, no. 2, pp. 649–658, Feb. 2007.
[29] A. Ribeiro, X. Cai, and G. B. Giannakis, "Symbol error probabilities for general Cooperative links," *IEEE Trans. Wireless Commun.*, vol. 4, no. 3, pp. 1264–1273, May 2005.
[30] Z. Wang and G. B. Giannakis, "A simple and general parameterization quantifying performance in fading channels," *IEEE Trans. Commun.*, vol. 51, no. 8, pp. 1389–1398, Aug. 2003.
[31] S. Boyd and L. Vandenberghe, *Convex Optimization*. Cambridge, U.K.: Cambridge Univ. Press, 2004.
[32] A. A. Kilbas and M. Saigo, *H-Transforms: Theory and Applications*. New York, NY, USA: CRC Press, 2004.

ALI CHELLI (S'08–M'12) was born in Sfax, Tunisia. He received the B.Sc. degree in communications from the Ecole Superieure des Communications de Tunis, in 2005, and the M.Sc. and Ph.D. degrees in information and communication technology from the University of Agder, Norway, in 2007 and 2013, respectively. He served as a Post-Doctoral Fellow with the King Abdullah University of Science and Technology. He is currently a Post-Doctoral Fellow with the Norwegian University of Science and Technology, Trondheim, Norway. His research interests include wireless communication theory with a focus on performance analysis of cooperative relaying, vehicle-to-vehicle communications, game theory, and channel modelling.

KIMMO KANSANEN received the M.Sc degree in electrical engineering and the Dr. Tech. degree from the University of Oulu, Finland, in 1998 and 2005, respectively. He was a Research Scientist and a Project Manager with the Centre for Wireless Communications, University of Oulu. Since 2006, he has been with the Norwegian University of Science and Technology, Trondheim, Norway, where he has also been a Professor since 2016. His research interests are communications and signal processing. He is in the Editorial Board of *Elsevier Physical Communications*.

MOHAMED-SLIM ALOUINI (S'94–M'98–SM'03–F'09) was born in Tunis, Tunisia. He received the Ph.D. degree in electrical engineering from the California Institute of Technology, Pasadena, CA, USA, in 1998. He served as a Faculty Member with the University of Minnesota, Minneapolis, MN, USA, and Texas A&M University at Qatar, Doha, Qatar, before joining the King Abdullah University of Science and Technology, Thuwal, Saudi Arabia, as a Professor of electrical engineering in 2009. His current research interests include the modeling, design, and performance analysis of wireless communication systems.

ILANGKO BALASINGHAM (S'91–M'98–SM'11) received the M.S. and Ph.D. degrees in signal processing from the Department of Electronics and Telecommunications, Norwegian University of Science and Technology (NTNU), Trondheim, Norway, in 1993 and 1998, respectively, and the M.S. degree from the Department of Electrical and Computer Engineering, University of California at Santa Barbara, Santa Barbara, CA, USA. Since 2002, he has been a Senior Research Scientist with the Intervention Center, Oslo University Hospital, Oslo, Norway, where he heads the Wireless Sensor Network Research Group. Since 2006, he has been a Professor in signal processing in medical applications with NTNU. His research interests include super-robust short range communications for both in-body and onbody sensors, body area sensor network, microwave short range sensing of vital signs, short range localization and tracking mobile sensors, and nanoneural communication networks.